

# Zero-Shot Object Re-Identification in Egocentric Kitchen Videos via Multi-Stage SAM3 Feature Fusion

Dmytro Klepachevskyi Alexander Wong Sirisha Rambhatla Yuhao Chen  
University of Waterloo  
Waterloo, Ontario, Canada

{dklepachevskyi, alexander.wong, sirisha.rambhatla, yuhao.chen1}@uwaterloo.ca

## Abstract

Object re-identification (ReID) in egocentric kitchen videos is challenging due to rapid viewpoint changes, frequent occlusions, cluttered scenes, and large intra-class appearance variations. Objects may leave and re-enter the field of view, and the large diversity of instances with limited annotations makes supervised ReID difficult to scale, motivating zero-shot approaches. We study zero-shot object ReID on the EPIC-Kitchens benchmark, where the goal is to match active food and kitchen-tool instances across frames using only pre-trained visual features. We first evaluate five state-of-the-art feature extractors, including Vision-Language Models (VLMs) - CLIP, DINOv2, DreamSim, I-JEPA, and SAM3 - and show that zero-shot methods fail, with the best baseline achieving only 45.3% mAP. We then propose an Enhanced SAM3 ReID Pipeline, a zero-shot multi-stage method built around SAM3 segmentation as the core component. Stage 1 uses SAM3 to suppress background clutter. Stage 2 fuses embeddings from SAM3, DINOv2, and CLIP into a single L2-normalized descriptor. Stage 3 augments cosine similarity with mask-shape IoU for geometric consistency, and Stage 4 applies  $k$ -reciprocal re-ranking. The full pipeline improves performance by 7.5% mAP to 52.8%.

## 1. Introduction

Knowing *which* specific food item a person is handling - and being able to find it again later in the video - is a prerequisite for a broad class of applications. Automated dietary assessment systems must link the same apple or bowl of pasta across multiple frames to estimate portions and log nutrition [7, 13]. Physically-grounded 3D food reconstruction, requires matching the same food object across viewpoints before any volume estimation can occur. Fine-grained cooking activity recognition [5, 11] depends on knowing which ingredient is being cut, stirred, or plated at

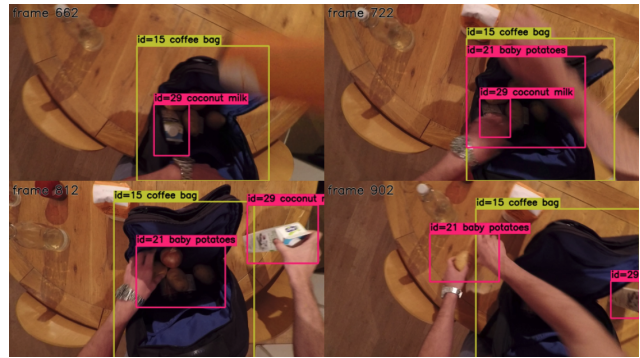


Figure 1. Example of a video sequence from EPIC-KITCHENS dataset with annotated objects. The ID of the same object is preserved across all the frames.

each moment - a question that is fundamentally one of object identity rather than category. Yet despite this shared dependency, *object re-identification* (ReID) in kitchen video has received almost no dedicated study.

We address this gap. Given a query crop of a kitchen object - a bowl, a spatula, a tomato - the ReID task asks: can a system retrieve all other crops of the *same physical instance* across the video? We study this in the zero-shot setting on EPIC-Kitchens [4], the largest egocentric kitchen benchmark, where ground-truth bounding-box tracks define object identity but no identity-labelled training data is used.

This can play a crucial role in robotics applications, where a camera-based robot should be able to retrieve and find objects given a query.

Person ReID [14–17] and Vehicle ReID [1, 12] has been thoroughly studied, but generalizable object ReID in kitchen settings introduces a distinct set of challenges. First, objects are *semantically diverse*: a “cutting board” or a “handful of pasta” has no canonical orientation or colour, unlike a pedestrian. Second, objects experience *extreme partial occlusion* as hands manipulate them, and backgrounds are cluttered with other food and surfaces.

Third, and most importantly for this work, while ground-truth bounding-box tracks are available for evaluation, no identity-labelled kitchen-object data is used for training - all models are used zero-shot.

Recent advances in vision-language pre-training and self-supervised learning have produced powerful state-of-the-art visual encoders. CLIP [9] aligns visual and linguistic semantics, DINOv2 [8] learns instance-discriminative patch features, DreamSim [6] targets human perceptual similarity, I-JEPA [2] predicts latent representations, and SAM3 [10] extends Segment Anything to video with a powerful vision-language backbone. Each encoder captures a different facet of visual appearance, motivating ensemble strategies.

In this paper we make three contributions:

1. We establish the first systematic zero-shot ReID benchmark on EPIC-Kitchens (Figure 1), evaluating six state-of-the-art encoders under a unified protocol (§3).
2. We design and ablate a four-stage Enhanced SAM3 pipeline (Figure 2) (background removal, multi-model fusion, mask-IoU reweighting, k-reciprocal re-ranking), which achieves mAP of 0.528, which leads to an improvement of 7.5%.
3. Guided by the ablation, we also propose a lightweight *Multi-Model Fusion* baseline that achieves mAP of 0.460 - a 0.7% relative improvement over the best other single encoder baseline - using only L2-normalised feature concatenation on unmodified crops (§3).

Our findings have a clear practical message: a complex segmentation-based preprocessing pipeline shows significant improvements in zero-shot egocentric ReID, and diverse feature ensembles on natural crops set up strong baseline results.

## 2. Methodology

### 2.1. Method Motivation

Standard multi-object trackers handle short-term occlusion well but break down across long temporal gaps, exactly the scenario that arises when a pot is moved off-screen or an ingredient is set aside and retrieved later. Closing this gap requires a retrieval-based approach: given a crop of an object at one moment in time, find all other crops of the same object in a large gallery, regardless of when or how they appear.

Our work addresses this gap in a zero-shot setting, without any fine-tuning on kitchen data. This choice is deliberate: annotated identity tracks in egocentric kitchen video [5] are scarce and expensive to produce, so a practical system must generalize from large-scale pre-trained representations. We systematically evaluate which state-of-the-art visual encoders transfer best to this domain, and we design a post-processing pipeline that squeezes additional performance from these frozen features through background

suppression, complementary fusion, and graph-based re-ranking.

### 2.2. Problem Formulation

Given a video with  $N$  ground-truth bounding-box crops  $\mathcal{X} = \{x_i\}_{i=1}^N$ , each assigned a track identity  $y_i \in \{1, \dots, K\}$ , we split  $\mathcal{X}$  into a gallery set  $\mathcal{G}$  (75%) and a query set  $\mathcal{Q}$  (25%) by stratified random sampling. For each query  $q \in \mathcal{Q}$  we rank all gallery items  $g \in \mathcal{G}$  by similarity and evaluate with mAP and Top- $k$  metrics. All methods are *zero-shot*: no identity labels are used at any stage.

### 2.3. Single-Model Baselines

We extract a fixed-size embedding  $\phi(x) \in \mathbb{R}^d$  from each crop using six encoders, all used off-the-shelf with no fine-tuning. The encoders span a broad design space, from language-supervised to purely self-supervised models, and from general-purpose to task-specific backbones.

We begin with **CLIP ViT-B/32** [9], which encodes each crop with the visual branch of a vision-language model pre-trained on 400M image-text pairs, producing a CLS-token embedding of dimension  $d = 512$ . As a purely self-supervised alternative we evaluate **DINOv2 ViT-B/14** [8], trained with knowledge distillation on a curated 142M-image corpus ( $d = 768$ ), and its successor **DINOv3 ViT-B/16**, which extends the same recipe to a larger and more diverse pre-training set. A qualitatively different signal comes from **DreamSim** [6], a perceptual similarity model that combines CLIP, DINO, and OpenCLIP embeddings via a learned MLP head trained on human triplet judgements, making it sensitive to the kind of holistic appearance differences that matter to human observers. We also include **I-JEPA ViT-H** [2], which learns by predicting latent patch representations from masked context regions without any pixel-level reconstruction; features are obtained by mean-pooling patch tokens ( $d = 1280$ ). Finally, **SAM3 ViT-H** [10] is the vision backbone of the Segment Anything 3 model, pre-trained on large-scale video data; we extract vision features and apply global average pooling ( $d = 256$ ). For all encoders, gallery items are ranked by cosine similarity to the query embedding.

### 2.4. Enhanced SAM3 Pipeline

Error analysis of the single-model baselines reveals three recurring failure reasons: cluttered backgrounds that make embeddings noisy with irrelevant texture, the limited coverage of any individual pre-trained model, and cosine similarity scores that ignore the geometric shape of the object. No single encoder addresses all three simultaneously, which motivates a pipeline that tackles each failure reason. Building on these observations, we propose a four-stage pipeline that combines background suppression, multi-model feature fusion, geometry-aware scoring, and graph-based re-

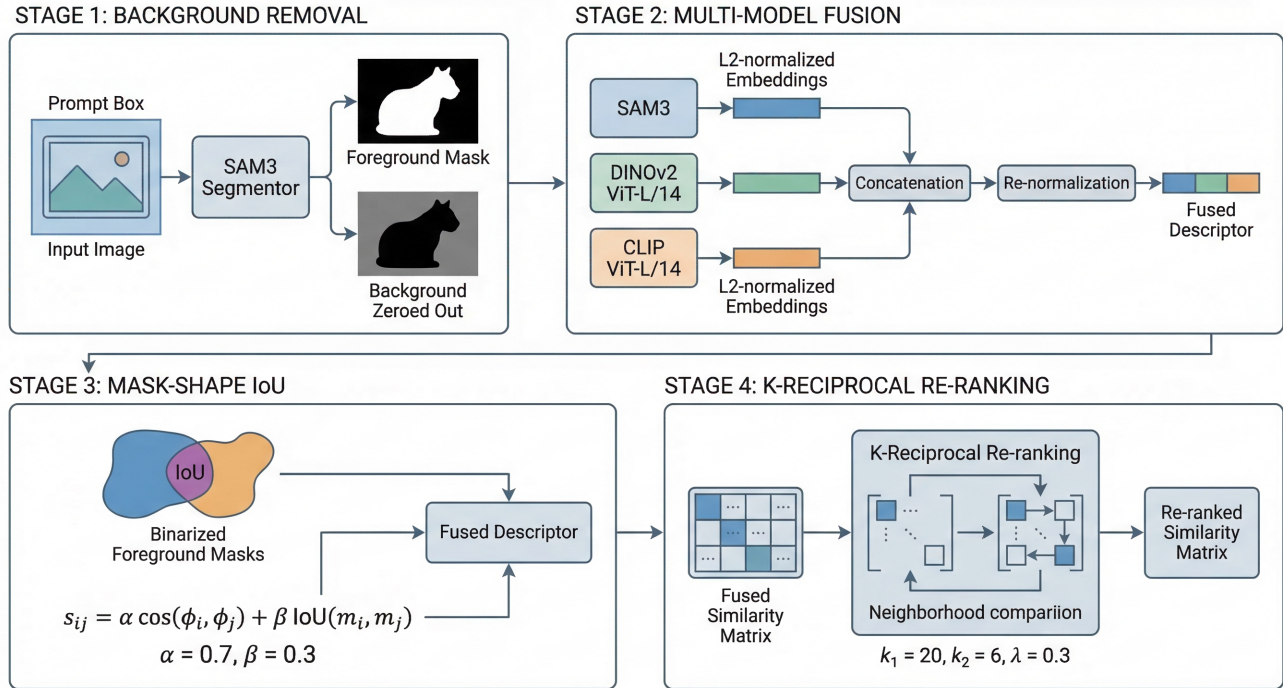


Figure 2. Our 4-staged enhanced SAM3 method with feature fusion. The first stage incorporates background removal to get a foreground mask. The second stage uses a multi-model fusion of three embeddings (SAM3, DINOv2, CLIP). The Stage 3 uses cosine similarity with an IoU term. The Stage 4 applies K-reciprocal re-ranking to the fused similarity matrix.

ranking. Each stage targets a distinct source of error in zero-shot kitchen ReID, and together they form a modular system whose components can be used independently, as confirmed by our ablation study (Table 2).

The first stage addresses the fact that kitchen crops often contain cluttered backgrounds — counter-tops, appliances, and hands — that introduce spurious texture signals into the embedding. For each crop, we invoke the SAM3 [10] segmentor with a prompt box covering the full crop extent (normalised to  $[0, 1]$ ) to obtain a binary foreground extent  $m_i \in \{0, 1\}^{H \times W}$ . The background pixels are zeroed out before any feature is extracted, so the encoder focuses exclusively on the object of interest.

In the second stage we compensate for the limited coverage of any single pre-trained model by fusing three complementary encoders. L2-normalised embeddings from SAM3 ViT-H, DINOv2 ViT-L/14, and CLIP ViT-L/14 are concatenated along the feature dimension and re-normalised to unit length, yielding a single fused descriptor:

$$\Phi_i = \ell_2([\ell_2(\phi_i^{\text{SAM3}}) \parallel \ell_2(\phi_i^{\text{DINOv2}}) \parallel \ell_2(\phi_i^{\text{CLIP}})]). \quad (1)$$

SAM3 provides instance-level spatial detail, DINOv2 contributes robust semantic structure, and CLIP supplies open-vocabulary object-class information, making the three encoders largely complementary.

The third stage enriches the pairwise similarity score with a geometric signal derived from the foreground masks produced in Stage 1, using the fused descriptor  $\Phi_i$  from Eq. 1. Pure cosine similarity treats two crops as equally similar regardless of whether their object silhouettes agree. We replace it with a weighted combination:

$$s_{ij} = \alpha \cos(\Phi_i, \Phi_j) + \beta \text{IoU}(m_i, m_j), \quad (2)$$

where the IoU term rewards pairs whose foreground shapes overlap well and penalises matches that are visually similar in texture but geometrically inconsistent. We set  $\alpha = 0.7$  and  $\beta = 0.3$  throughout all experiments.

The fourth and final stage applies k-reciprocal re-ranking [18] to the full pairwise similarity matrix defined by Eq. 2. Re-ranking exploits the mutual-neighbour structure of the gallery: two items are up-weighted if they appear in each other’s top- $k$  neighbour lists, which is a strong indicator of a true match. We use the hyperparameters  $k_1 = 20$ ,  $k_2 = 6$ , and  $\lambda = 0.3$ , following standard practice in person ReID literature.

## 2.5. Multi-Model Fusion on Natural Crops

Motivated by the ablation, we propose another simple pipeline for results improvement: *fuse complementary en-*

coders directly on the original, unmodified crop. Given feature parts  $\{\phi_m(x)\}_{m=1}^M$  from  $M$  encoders, we compute:

$$\Phi(x) = \ell_2([\ell_2(\phi_1(x)) \parallel \dots \parallel \ell_2(\phi_M(x))]), \quad (3)$$

where  $\parallel$  denotes concatenation and  $\ell_2$  denotes row-wise L2 normalisation. We evaluate all subsets of  $\{\text{DINOv2}, \text{DreamSim}, \text{CLIP ViT-L/14}\}$  and additionally test *Average Query Expansion* (AQE, [3]) with  $k = 10$ : each query is replaced by the mean of itself and its top- $k$  gallery neighbours before final ranking.

### 3. Experiments

In this section, we provide both qualitative and quantitative results of our experiments. Qualitatively, we compare how different baseline models track an object ID in a video sequence. We provide qualitative results for 3 best baseline models (CLIP, DINOv2, SAM3) and for two proposed methods by our study — Enhanced SAM3 pipeline and a Multi-Model Fusion method.

#### 3.1. Dataset

We evaluate our pipeline on 10 mostly overcrowded with objects video sequences from the EPIC-KITCHENS[4] dataset (Figure 1). Ground-truth bounding-box tracks from the MOT-format annotations define object identities. Crops smaller than 32 px in either dimension are discarded. A 5% padding is applied around each bounding box before cropping. The 75%/25% gallery/query split is fixed for all experiments.

#### 3.2. Metrics

For each query crop, all gallery items are ranked by cosine similarity to the query embedding. We report two complementary metrics:

Mean Average Precision (mAP) measures the quality of the full ranking. For a query  $q$  with  $R$  relevant items in the gallery, Average Precision is defined as:

$$\text{AP}(q) = \frac{1}{R} \sum_{k=1}^N P(k) \cdot \text{rel}(k), \quad (4)$$

where  $N$  is the gallery size,  $P(k)$  is the precision at cut-off  $k$ , and  $\text{rel}(k) \in \{0, 1\}$  indicates whether the item ranked at position  $k$  is a true match. mAP averages AP over all  $Q$  queries:

$$\text{mAP} = \frac{1}{Q} \sum_{q=1}^Q \text{AP}(q). \quad (5)$$

mAP is the area under the Precision-Recall curve, rewarding systems that place all true matches at the top of the ranked list. Unlike Top- $K$ , mAP penalises false positives

anywhere in the ranking, making it the primary metric for retrieval evaluation.

Cumulative Matching Characteristic (CMC) at Top-1, Top-3, and Top-5 measures recall: the fraction of queries for which at least one true match appears within the top  $K$  retrieved results.

The two metrics capture different failure modes: a system can achieve high Top-1 by consistently finding one easy match, while mAP exposes whether it retrieves *all* instances of an identity. We use both to provide a complete picture of retrieval performance.

#### 3.3. Single-Model Baseline Results

Table 1 summarises all single-model baselines on 10 mostly overcrowded sequences. DreamSim achieves the best mAP (0.453) and Top-1 (85.2%). I-JEPA attains the third-highest Top-1 (81.7%) despite weaker mAP, suggesting it is good at nearest-neighbour retrieval but less precise at ranking multiple positives. SAM3, having a powerful backbone, ranks second after DreamSim; its features which are optimised for segmentation work fine for instance discrimination as well. DINOv3, evaluated on ten sequences, performs poorly (mAP of 0.110), suggesting that its larger pre-training distribution does not transfer well to close-range kitchen objects without fine-tuning.

Table 1. Single-model zero-shot ReID in comparison to our Enhanced SAM3 method on EPIC-Kitchens dataset.

Model	mAP	Top-1	Top-3	Top-5
CLIP ViT-B/32	0.355	0.773	0.889	0.926
DINOv2 ViT-B/14	0.416	0.774	0.903	0.939
DINOv3 ViT-B/16	0.110	0.742	0.891	0.929
I-JEPA ViT-H	0.321	0.817	0.913	0.942
SAM3 ViT-H	0.451	0.872	<b>0.946</b>	<b>0.955</b>
DreamSim	0.453	0.852	0.942	0.954
Ours Enhanced SAM3	<b>0.528</b>	<b>0.893</b>	0.907	<b>0.955</b>

#### 3.4. Enhanced SAM3 pipeline

The full pipeline (all stages enabled) achieves mAP of 0.528 (Table 1) and Top-1 of 0.893 - which gives an improvement of 7.5% of mAP metric, and 2.1% of Top-1 metric over the best single-model baseline (DreamSim). Qualitative analysis (Figure 3) reveals that for given queries, the developed enhanced SAM3 Feature Fusion method significantly improves the results, where it manages to achieve all 5 correct retrievals, whereas the other methods fail at least 2 times.

#### 3.5. Ablation Study

Table 2 shows the full ablation of the four-stage Enhanced SAM3 pipeline (shown in Figure 2). We quantitatively confirm that removal of the feature fusion part hurts the most

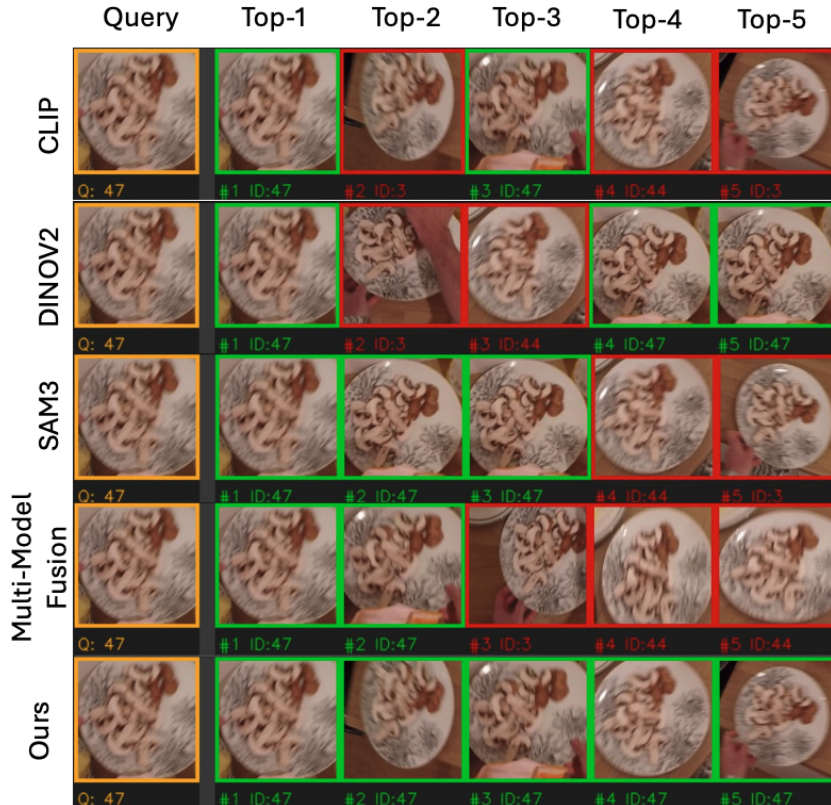


Figure 3. Qualitative results. We evaluate three baseline methods (CLIP, DINOv2, SAM3) along with our methods — Multi-Model Fusion and Enhanced SAM3 Fusion method. The evaluation is presented given the same query object and Top-5 predictions. The analysis shows that 4 methods make at least 2 mistakes in the object ID assignment, while our SAM3 enhanced pipeline make all 5 correct predictions.

(5.5% drop of mAP), whereas removal of every single component hurts the performance, which proves that all 4 stages overall improve the performance.

Table 2. Enhanced SAM3 pipeline ablation on EPIC-Kitchens dataset. Each row disables one stage; ✓ = enabled.

BG	Fusion	MaskIoU	Rerank	mAP	Top-1	Top-3
✓	✓	✓	✓	<b>0.528</b>	<b>0.893</b>	<b>0.907</b>
	✓	✓	✓	0.501	0.842	0.863
		✓	✓	0.473	0.827	0.849
	✓		✓	0.511	0.884	0.897
	✓	✓		0.498	0.835	0.862

### 3.6. Multi-Model Fusion Results

Table 3 reports fusion experiments on ten sequences from EPIC-Kitchens dataset. All runs use natural, unmodified crops. DINOv2+DreamSim already outperforms every single baseline encoder (mAP of 0.455). Adding CLIP provides a marginal further gain in mAP (0.458) with no significant Top-1 change. Average Query Ex-

pansion (AQE,  $k = 10$ ) improves mAP slightly (0.460 with 3-way fusion) but reduces Top-1 (0.801 vs. 0.825), as expanded queries become less discriminative in the small gallery setting. The best balanced operating point is **DINOv2+DreamSim+CLIP** without AQE: mAP 0.458, Top-1 82.5%.

Table 3. Multi-model fusion on ten sequences of EPIC-Kitchens dataset. All encoders run on original crops.

Models	QE	mAP	Top-1	Top-3
DreamSim		0.433	0.822	0.932
DINOv2+DreamSim		0.455	0.820	0.934
DINOv2+DreamSim+CLIP		0.458	<b>0.825</b>	<b>0.936</b>
DINOv2+DreamSim	10	0.447	0.789	0.879
DINOv2+DreamSim+CLIP	10	<b>0.460</b>	0.801	0.877

### 3.7. Conclusion

We presented a study of zero-shot object re-identification in egocentric kitchen videos on EPIC-Kitchens. Across six state-of-the-art encoders, DreamSim and SAM3 emerge as

the strongest single-model baselines (mAP  $\approx 0.45$ ), while encoders with larger pre-training corpora (DINOv3) do not necessarily transfer better to close-range kitchen objects. Our four-stage Enhanced SAM3 pipeline - background removal, multi-model embedding fusion, mask-IoU reweighting, and k-reciprocal re-ranking - achieves mAP 0.528, a relative gain of 7.5% over the best single encoder. A lightweight Multi-Model Fusion baseline (DINOv2+DreamSim+CLIP) reaches mAP 0.458, which runs 5x times faster in wall-clock time per each query than the SAM3 enhanced method. Ablations confirm that each stage contributes independently. These results establish strong zero-shot baselines for kitchen-object ReID and highlight that background removal, complementary feature ensembling, and geometric re-ranking are beneficial stages for future work in egocentric instance retrieval.

## References

- [1] Ali Amiri, Aydin Kaya, and Ali Seydi Keceli. A comprehensive survey on deep-learning-based vehicle re-identification: Models, data sets and challenges, 2024. 1
- [2] Mahmoud Assran, Quentin Duval, Ishan Misra, Piotr Bojanowski, Pascal Vincent, Michael Rabbat, Yann LeCun, and Nicolas Ballas. Self-supervised learning from images with a joint-embedding predictive architecture. In *CVPR*, 2023. 2
- [3] Ondrej Chum, James Philbin, Josef Sivic, Michael Isard, and Andrew Zisserman. Total recall: Automatic query expansion with a generative feature model for object retrieval. In *ICCV*, 2007. 4
- [4] Dima Damen, Hazel Doughty, Giovanni Maria Farinella, Sanja Fidler, Antonino Furnari, Evangelos Kazakos, Davide Moltisanti, Jonathan Munro, Toby Perrett, Will Price, and Michael Wray. Scaling egocentric vision: The EPIC-Kitchens dataset. In *ECCV*, 2018. 1, 4
- [5] Dima Damen, Hazel Doughty, Giovanni Maria Farinella, Antonino Furnari, Evangelos Kazakos, Jian Ma, Davide Moltisanti, Jonathan Munro, Toby Perrett, Will Price, and Michael Wray. Rescaling egocentric vision: Collection, pipeline and challenges for EPIC-KITCHENS-100. *IJCV*, 130(1):33–55, 2022. 1, 2
- [6] Stephanie Fu, Netanel Tamir, Shobhita Sundaram, Lucy Chai, Richard Zhang, Tali Dekel, and Phillip Isola. DreamSim: Learning new dimensions of human visual similarity using synthetic data. In *NeurIPS*, 2023. 2
- [7] Wenyang Jia, Yuecheng Li, Ruowei Qu, Thomas Baranowski, Lora E. Burke, Hong Zhang, Yicheng Bai, Juliet M. Mancino, Guizhi Xu, Zhi-Hong Mao, and Mingui Sun. Automatic food detection in egocentric images using artificial intelligence technology. *Public Health Nutrition*, 22(7):1168–1177, 2019. 1
- [8] Maxime Oquab, Timothée Darcet, Théo Moutakanni, Huy V. Vo, Marc Szafraniec, Vasil Khalidov, Pierre Fernandez, Daniel Haziza, Francisco Massa, Alaaeldin El-Nouby, Mahmoud Assran, Nicolas Ballas, Wojciech Galuba, Russell Howes, Po-Yao Huang, Shang-Wen Li, Ishan Misra, Michael Rabbat, Vasu Sharma, Gabriel Synnaeve, Hu Xu, Hervé Jégou, Julien Mairal, Patrick Labatut, Armand Joulin, and Piotr Bojanowski. DINOv2: Learning robust visual features without supervision. *Trans. Mach. Learn. Res.*, 2024. 2
- [9] Alec Radford, Jong Wook Kim, Chris Hallacy, Aditya Ramesh, Gabriel Goh, Sandhini Agarwal, Girish Sastry, Amanda Askell, Pamela Mishkin, Jack Clark, Gretchen Krueger, and Ilya Sutskever. Learning transferable visual models from natural language supervision. In *Int. Conf. Mach. Learn.*, 2021. 2
- [10] Nikhila Ravi, Valentin Gabeur, Yuan-Ting Hu, Ronghang Hu, Chaitanya Ryali, Tengyu Ma, Haitham Khedr, Roman Rädle, Chloe Rolland, Laura Gustafson, Eric Mintun, Junting Pan, Kalyan Vasudev Alwala, Nicolas Carion, Chao-Yuan Wu, Ross Girshick, Piotr Dollár, and Christoph Feichtenhofer. SAM 3: Segment anything in images and videos. *arXiv preprint arXiv:2511.16719*, 2025. 2, 3
- [11] Marcus Rohrbach, Sikandar Amin, Mykhaylo Andriluka, and Bernt Schiele. A database for fine grained activity detection of cooking activities. In *CVPR*, pages 1194–1201, 2012. 1
- [12] Fei Shen, Xiaoyu Du, Liyan Zhang, Xiangbo Shu, and Jinhui Tang. Triplet contrastive representation learning for unsupervised vehicle re-identification, 2023. 1
- [13] Quin Thames, Arjun Karapur, Wade Norris, Fangting Xia, Liviu Panait, Tobias Weyand, and Jack Sim. Nutrition5k: Towards automatic nutritional understanding of generic food. In *CVPR*, pages 8903–8911, 2021. 1
- [14] Changshuo Wang, Xingyu Gao, Meiqing Wu, Siew-Kei Lam, Shuting He, and Prayag Tiwari. Looking clearer with text: A hierarchical context blending network for occluded person re-identification. *IEEE Transactions on Information Forensics and Security*, 20:4296–4307, 2025. 1
- [15] Haoxuan Xu, Bo Li, and Guanglin Niu. Identity-aware feature decoupling learning for clothing-change person re-identification, 2025.
- [16] Bin Yang, Jun Chen, and Mang Ye. Shallow-deep collaborative learning for unsupervised visible-infrared person re-identification. In *Proceedings of the IEEE/CVF Conference on Computer Vision and Pattern Recognition (CVPR)*, pages 16870–16879, 2024.
- [17] Ruiheng Zhang, Zhe Cao, Yan Huang, Shuo Yang, Lixin Xu, and Min Xu. Visible-infrared person re-identification with real-world label noise. *IEEE Transactions on Circuits and Systems for Video Technology*, 35(5):4857–4869, 2025. 1
- [18] Zhun Zhong, Liang Zheng, Donglin Cao, and Shaozi Li. Re-ranking person re-identification with k-reciprocal encoding. In *CVPR*, 2017. 3